

Experimental Study of Frequency-Change-Type Force Sensor 周波数変化型力センサの実験的検討

Sumio Sugawara, Ryo Sasada[†], Yu Kajiwara (Faculty of Sci. and Tech., Ishinomaki Senshu Univ.)

菅原 澄夫, 佐々田 涼[‡], 梶原 優 (石巻専修大 理工)

1. Introduction

A high-sensitive force sensor that utilizes the resonance frequency change of a bending vibrator by axial force is expected as a new small low-cost sensor using MEMS technology. The authors have developed a new flat force sensor using an out-of-plane mode as the sensor.¹⁾ The developed sensor can be applied to an acceleration sensor²⁻⁷⁾ and also to an inclination angle sensor.⁸⁾ The various force sensors using the same principle have been proposed.^{9,10)} Then the characteristics of these sensors were theoretically compared with each other from the standpoint of sensitivity and displacements at fixed portions.¹¹⁾ However, the experimental investigation is not realized yet.

In this study, the characteristics of the various force sensors are analyzed by the finite-element method, and then inspected experimentally.

2. Structure of Sensor

The various force sensors are shown in Fig. 1. These sensors utilize the phenomenon that the resonance frequency of a vibrating long arm is changed by an axial force in the y-direction, and detect the axial force F applied in the y-direction at both ends as a change in the resonance frequency.

Fig. 1(a) shows the newly developed structure utilizing an out-of-plane mode.¹⁾ The sensor vibrates in the z-direction as shown in Fig. 2(a). Only one vibrating long arm is used from the standpoint of high sensitivity. Using the long arm, the axial force is detected by a piezoelectric method. In this structure, two short arms are arranged on the left and right sides at both ends of the long arm and are used for balancing the vibration energy. With such a device, the force sensor is not affected by fixation and has a high-quality factor because the displacements at both ends are markedly reduced.

Figs. 1(b) and 1(c) show the structures utilizing an in-plane mode. The device applied to Fig. 1(a) is also applied to these structures. The sensors vibrate in the x-direction, which is horizontal to their surfaces, as shown in Figs. 2(b) and 2(c). Figs. 1(d) and 1(e) show the structures utilizing an in-plane mode in which two arms vibrate symmetrically as shown in Figs. 2(d) and

2(e). In these structures, the two long arms are used for reducing the displacements at both ends by using a symmetrical vibration.

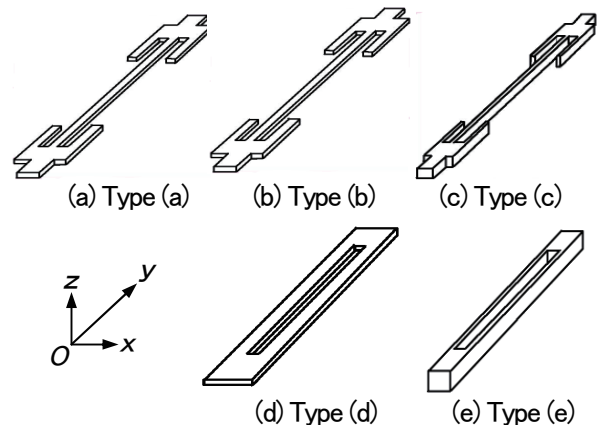


Fig. 1. Various structures of force sensor.

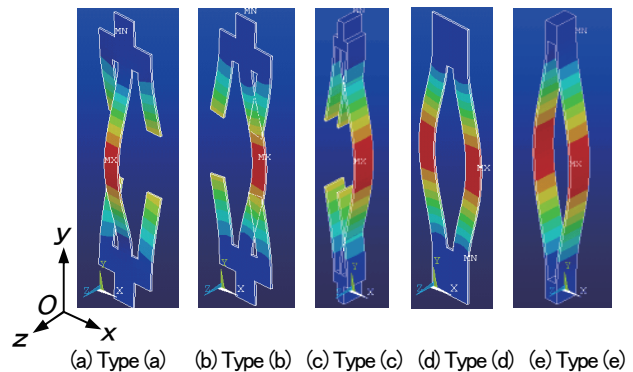


Fig. 2. Vibration modes of force sensor.

3. Characteristics of Sensor

The sensor material is stainless steel (SUS304). Young's modulus, Poisson's ratio, and the density of the material are $E=1.99 \times 10^{11} \text{N/m}^2$, $\sigma=0.34$ and $\rho=7.9 \times 10^3 \text{kg/m}^3$, respectively. The dimensions of the sensors have already designed.⁵⁾ These sensors are fabricated with large dimensions for ease of handling in this case, because the sensors may be miniaturized in the future using a single crystal. Ansys 11.0 of CyberNet System is used as the analytical software.

Because the sensor is fixed at both ends, the displacements at both ends are analyzed by the finite-element method and reduced by modifying the shape of the sensor base. The displacements u_i

E-mail address: ssumio@isenshu-u.ac.jp

($i=x, y, z$) at the base end of the sensor were analyzed as the ratio u_i/u_{i0} to the displacement u_{i0} and listed in **Table I**. Here, u_{i0} is the maximum displacement in the i -direction at the central portion of the long arm. The values of u_i/u_{i0} in the sensors of types (a) and (e) are less than 10^{-3} . Therefore these structures are suitable for the force sensor. The values which are smaller than 10^{-7} are shown as zero in the table.

Table I. Displacement ratios f sensor.

Type	u_i/u_{i0} at center portion ($\times 10^{-3}$)			u_i/u_{i0} at edge portion ($\times 10^{-3}$)		
	u_x/u_{x0}	u_y/u_{y0}	u_z/u_{z0}	u_x/u_{x0}	u_y/u_{y0}	u_z/u_{z0}
(a)	0	0	-0.355	0	0	-0.702
(b)	0.880	-2.10	0	0.880	-8.44	0
(c)	-0.326	0	0	-0.326	-4.73	0
(d)	0	-6.64	0	-0.344	-6.89	0
(e)	0	-0.179	0	0	-0.179	0

Then, the axial force in the y-direction is applied to both ends of the sensor, and the change Δf ($=f_0'-f_0$) in the resonance frequency f_0 was also analyzed. Here f_0' is the resonance frequency when the axial force is applied. The value of Δf becomes positive in the case of a tension of $F>0$, and becomes negative in the case of a compressive force of $F<0$. **Fig. 3** shows the calculated relationship between F and $\Delta f/f_0$, and the characteristics are all linear in the range of a given force. As a result, the sensors of types (a), (c) and (e) are more sensitive than the other types.

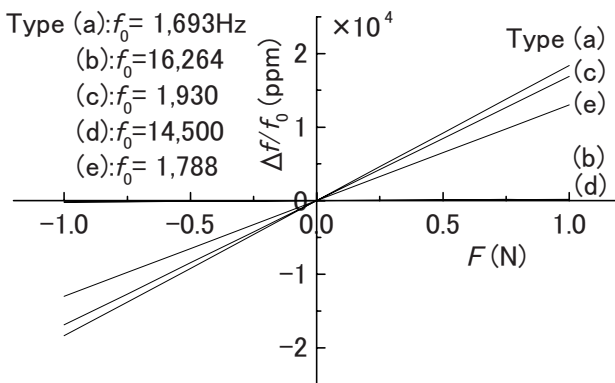


Fig. 3 Characteristics of $F-\Delta f/f_0$, in the case of the sensor without piezoelectric ceramics.

Fig. 4 shows the characteristics of the sensor with piezoelectric ceramics for driving. The measured characteristics agree with the calculated ones. Because of the bonded piezoelectric ceramics, the sensor sensitivity is reduced to about half of the sensitivity of **Fig. 3**. The sensor of type (a) is preferable because of its flat and simple structure.

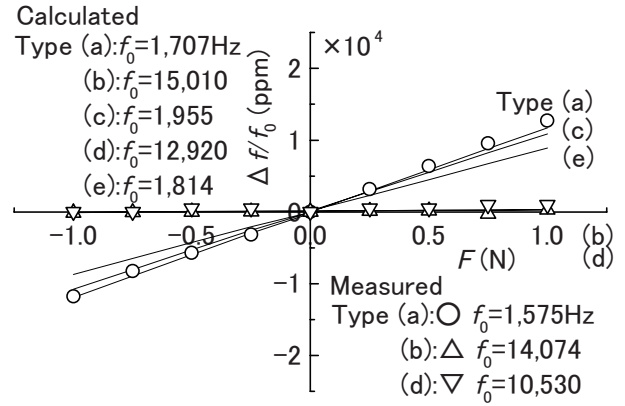


Fig. 4 Characteristics of $F-\Delta f/f_0$, in the case of the sensor with piezoelectric ceramics.

5. Conclusions

The analyzed characteristics of the various frequency-change-type force sensors were compared with the measured ones, and confirmed experimentally. The sensor of type (a) is the structure with high sensitivity and small displacements, and suitable for a MEMS device because of its flat and simple structure. This structure will be used as the acceleration and the inclination angle sensors in the future.

Acknowledgment

This work was partially supported by a Grant-in-Aid for Scientific Researches (No. 19560047 and No. 22560055) from the Japan Society for the Promotion of Science.

References

- 1) S. Sugawara, J. Takahashi, and Y. Tomikawa: Jpn J. Appl. Phys., **41** (2002) 3433.
- 2) S. Sugawara and J. Terada: Proc. 27th Symp. Ultrasonic Electronics, 2004, p. 185 [in Japanese].
- 3) J. Takahashi, S. Sugawara, and J. Terada: Jpn J. Appl. Phys., **42** (2003) 3124.
- 4) J. Takahashi, and S. Sugawara: Jpn J. Appl. Phys., **43** (2004) 3035.
- 5) S. Sugawara, H. Suzuki and T. Saito: Jpn J. Appl. Phys., **46** (2007) 4652.
- 6) S. Sugawara, and J. Koike: Jpn J. Appl. Phys., **47** (2008) 6578.
- 7) S. Sugawara and Y. Yajiwara: Jpn J. Appl. Phys., **49** (2010) 07HD02-1.
- 8) S. Sugawara, T. Watanabe, and J. Terada: Jpn J. Appl. Phys., **47** (2008) 4048.
- 9) L. Weisbond: US Patent 4,479,385 (1984).
- 10) J. Koitabashi, S. Kudoh, S. Okada, and Y. Tomikawa: Jpn. J. Appl. Phys., **41** (2002) 3403.
- 11) S. Sugawara, M. Yamakawa, and S. Kudo: Jpn J. Appl. Phys., **48** (2009) 07GF04-1.